Microfluidic chambers using fluid walls for cell biology

Cristian Soitu[a], Alexander Feuerborn[b,c], Ann Na Tan[b,c], Henry Walker[c], Pat A. Walsh[d], Alfonso A. Castrejón-Pita[e], Peter R. Cook[b,1], and Edmond J. Walsh[a,1]

[a]Department of Engineering Science, University of Oxford, OX2 0ES Oxford, United Kingdom; [b]Sir William Dunn School of Pathology, University of Oxford, OX1 3RE Oxford, United Kingdom; [c]IotaSciences Ltd., OX5 1PF Oxfordshire, United Kingdom; [d]Bernal Institute, School of Engineering, University of Limerick, Castletroy, V94 T9PX Limerick, Ireland; and [e]Department of Engineering Science, University of Oxford, OX1 3PJ Oxford, United Kingdom

Edited by David A. Weitz, Harvard University, Cambridge, MA, and approved May 21, 2018 (received for review March 28, 2018)

Many proofs of concept have demonstrated the potential of microfluidics in cell biology. However, the technology remains inaccessible to many biologists, as it often requires complex manufacturing facilities (such as soft lithography) and uses materials foreign to cell biology (such as polydimethylsiloxane). Here, we present a method for creating microfluidic environments by simply reshaping fluids on a substrate. For applications in cell biology, we use cell media on a virgin Petri dish overlaid with an immiscible fluorocarbon. A hydrophobic/fluorophilic stylus then reshapes the media into any pattern by creating liquid walls of fluorocarbon. Microfluidic arrangements suitable for cell culture are made in minutes using materials familiar to biologists. The versatility of the method is demonstrated by creating analogs of a common platform in cell biology, the microtiter plate. Using this vehicle, we demonstrate many manipulations required for cell culture and downstream analysis, including feeding, replating, cloning, cryopreservation, lysis plus RT-PCR, transfection plus genome editing, and fixation plus immunolabeling (when fluid walls are reconfigured during use). We also show that mammalian cells grow and respond to stimuli normally, and worm eggs develop into adults. This simple approach provides biologists with an entrée into microfluidics.

microfluidics | fluid walls | tissue culture | sessile drops | interfacial tension

Microfluidics addresses the manipulation of tiny volumes, typically less than 1 μL. Despite many proofs of concept involving common protocols in cell biology, uptake of microfluidics by biologists is limited. Some well-known and documented reasons include the cost and complexity of manufacture of microfluidic devices (which might involve soft lithography and clean rooms), concerns regarding biocompatibility (materials used for fabrication like polydimethylsiloxane and the associated solvents are not traditionally applied in cell biology), and the inaccessibility of cells after being introduced into enclosed spaces within devices. This prompts the development of many alternatives, including "open" and "paper-based" microfluidics (1).

Microtiter plates are widely used during liquid handling; each is essentially an array of miniature test tubes with 96, 384, or 1,536 wells in a uniform footprint, where wells have working volumes of ∼100 to 400, ∼15 to 150, or ∼3 to 10 μL, respectively. Arrays with more wells and volumes down to a few femtoliters have been developed (2, 3). Arrays of aqueous drops sitting on flat (usually patterned) surfaces and overlaid with an immiscible liquid to prevent evaporation have also been fabricated (4–9); in these, liquid walls/ceilings confine the aqueous phase. The burgeoning field of droplet-based microfluidics also uses fluid walls to confine liquids (10–12). However, compared with the widespread use of microtiter plates, few of these alternatives are incorporated into workflows in cell biology (13); consequently, most still involve volumes of many microliters.

A recent method termed Freestyle Fluidics allows fabrication of microfluidic circuits by dispensing cell media in a desired pattern on a Petri dish and overlaying it with an immiscible liquid (14). The aqueous phase is bounded by fluid walls—the interface between water and immiscible liquid. One of the resultant circuits was used in a chemotaxis experiment with bacterial cells, and several benefits compared with traditional circuits were demonstrated. Here, we also created microfluidics patterns with fluid walls. However, instead of depositing the aqueous phase in the desired pattern on the substrate and then overlaying the immiscible liquid, we simply reshaped the two fluids already on the substrate and allowed interfacial forces to build fluid walls accurately, reproducibly, and immediately. At the microscale, these fluid walls prove to be strong, pliant, and resilient; they morph above unchanging footprints when nanoliter volumes are added/removed. Although any 2D pattern can be made, we demonstrate the method and its versatility by creating analogs of a familiar experimental platform in cell biology, the microtiter plate. We show that mammalian cells grow and respond to stimuli normally and that worm eggs develop into adults. We also demonstrate many basic manipulations involved in cell biology (i.e., cell feeding, replating, cloning, and cryopreservation), plus some common downstream workflows (i.e., fixation/immunolabeling, cell lysis/RT-PCR, transfection/genome editing). Furthermore, we go beyond what is possible with existing microfluidics and reconfigure the fluidic structures in real time. We suggest that this method provides biologists with an easy entrée into microfluidics, without the usual expertise/equipment requirements, while also providing the freedom to create and reconfigure designs on demand.

Significance

Despite improvements in our ability to manipulate ever-smaller volumes, most workflows in cell biology still use volumes of many microliters. We describe a method for creating microfluidic arrangements containing submicroliter volumes. It exploits interfacial forces dominant at the microscale to confine liquids with fluid (not solid) walls. We demonstrate many basic manipulations required for cell culture and some widely used downstream workflows. The method eliminates many problems associated with the fabrication of conventional microfluidic devices, thereby providing a simple on-demand approach for fabrication of microfluidic devices using materials familiar to biologists.

Author contributions: C.S., A.F., P.R.C., and E.J.W. designed research; C.S., A.N.T., and E.J.W. performed research; H.W., P.A.W., and E.J.W. contributed new reagents/analytic tools; C.S., A.F., A.N.T., A.A.C.-P., P.R.C., and E.J.W. analyzed data; and C.S., A.F., P.A.W., A.A.C.-P., P.R.C., and E.J.W. wrote the paper.

Conflict of interest statement: Oxford University Innovation—the technology transfer company of the University of Oxford—has filed provisional patent applications on behalf of C.S., A.F., P.R.C., and E.J.W. partly based on this study. A.F., H.W, P.R.C., and E.J.W. each hold equity, or rights to equity, in Iota Sciences Ltd., a company that is exploiting this technology. Iota Sciences Ltd. provides a scholarship for C.S. and partially funds salaries and research of A.F., A.N.T., H.W., and P.A.W.

This article is a PNAS Direct Submission.

[1]To whom correspondence may be addressed. Email: peter.cook@path.ox.ac.uk or edmond.walsh@eng.ox.ac.uk.

This article contains supporting information online at www.pnas.org/lookup/suppl/doi:10.1073/pnas.1805449115/-/DCSupplemental.

Published online June 12, 2018.

Results

Methodology. Fig. 1*A* illustrates the fabrication of a 2 × 2 grid. The bottom of a standard polystyrene Petri dish is completely covered with cell medium, excess medium is removed, and the residual thin film is overlaid with an immiscible liquid. This overlay can be less dense than water, like a hydrocarbon. Perhaps counterintuitively, it can be denser, like FC40—a transparent fully fluorinated liquid (density 1.855 g/mL) that is widely used in droplet-based microfluidics; at the microscale, effects due to gravity and buoyancy become negligible, and interfacial forces pin the aqueous phase to the plastic. A hydrophobic and fluorophilic stylus with a conical tip made of polytetrafluoroethylene (Teflon) and held by a three-axis traverse (a "printer") is then lowered through both liquids until it just touches the dish. Because FC40 wets Teflon and polystyrene better than water, the tip (now coated with FC40) brings fluorocarbon down to wet the substrate. When the stylus moves laterally, the aqueous liquid is displaced from the surface to leave a track of FC40 pinned to plastic by interfacial forces. Drawing more lines creates a grid.

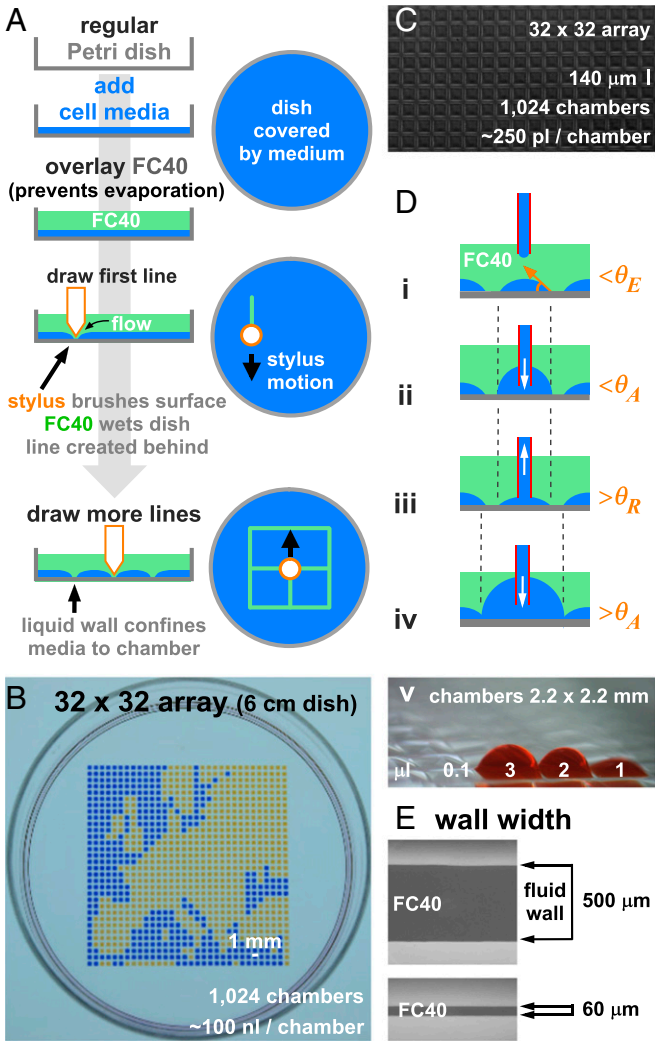

Fig. 1. Reverse printing. (*A*) Principle. A Petri dish is filled with DMEM plus 10% FBS, most medium is removed, and the residual thin film is overlaid with FC40 (shown in green). A hydrophobic stylus is lowered to touch the dish and to bring FC40 to the surface. As the stylus moves horizontally, medium is pushed aside and FC40 takes its place. This creates a track of FC40 pinned to the substrate and a liquid wall of FC40 dividing the aqueous layer. Drawing more lines creates a grid. (*B*) A 32 × 32 grid made in ~4 min. After printing, 70 nL of yellow or blue dye is added to each chamber. (*C*) A high-density grid made with a thin stylus (73% surface covered by medium). (*D*) Adding and subtracting medium. (*i*) The contact angle is $<\theta_E$ (~70°). (*ii*) Medium can be added without altering the footprint until θ_A is reached ($\theta_A > \theta_E$). (*iii*) Medium can be removed without altering the footprint until θ_R is reached (<3°). (*iv*) If θ_A is exceeded, the pinning line breaks and chambers merge. (*v*) Within limits imposed by θ_A and θ_E, grids are used like conventional plates; aqueous liquids are pipetted into (or out of) chambers through FC40 instead of air. Here, 1 to 3 µL of dye was added to chambers initially containing 0.1 µL of medium. Note that the maximum contact angle in the square drop with 3 µL was >70°. (*E*) Stylus width determines wall width. Lines were made using styli with wider and narrower tips than in *B*, and regions between chambers were imaged.

Grids with few or many chambers can be made in minutes (Fig. 1 *B* and *C*, *SI Appendix*, Fig. S1, and Movie S1); for example, chamber density in the grid in Fig. 1*C* is analogous to that of a microplate with 393,216 wells. Colored dyes are often pipetted into chambers to aid visualization; they play no role in stabilizing liquid structures. Individual chambers are used much like wells in conventional microplates; liquids are simply pipetted into (or removed from) them through FC40 instead of air (Fig. 1*D*). This can be achieved without altering the footprint on the dish. Consider a sessile water drop in air sitting on a standard polystyrene Petri dish. The drop is shaped like the cap of a sphere, and its footprint depends on the equilibrium contact angle (the angle θ_E, at the air–water–substrate interface) (15, 16). When tissue culture medium without serum replaces water, θ_E is ~50°, and θ_E increases to ~70° if FC40 replaces air (14). Slightly more medium can now be added without increasing the footprint, up to a limit determined by the advancing contact angle, θ_A ($\theta_A > \theta_E$); once θ_A is breached, footprint area increases. Similarly, when medium is removed, the footprint shrinks once the receding contact angle, θ_R, is reached. However, θ_R is <3°, so at least 95% of a 5-µL drop of medium can be removed without altering the footprint (14). Hereafter, medium with serum will generally be used, and θ_A becomes >70°. The significant difference between θ_A and θ_R allows the addition and removal of liquids above unchanging footprints (Fig. 1 *D*, *v*). The spacing between chambers can also be varied using styli with wider or narrower tips (Fig. 1*E*).

FC40 plays several additional roles. Fluorocarbons like FC40 were developed during the Manhattan Project as materials that could resist attack by highly reactive uranium hexafluoride; consequently, they are arguably the most inert liquids known. They are also the carrier fluid of choice in droplet-based microfluidics. In addition, FC40 carries the vital gases (O_2 and CO_2) so effectively that it has been used as a blood substitute (17), and FC40's close relatives have been used for liquid ventilation of human preterm neonates (18, 19). FC40 also prevents the underlying aqueous layer from evaporating (the solubility of water in FC40 is <7 ppm by weight at room temperature) while isolating each chamber from others in a dish (and from the surroundings), thereby preventing contamination and communication between adjacent chambers. For example, if bacteria are pipetted manually through FC40 into every second chamber in a grid, bacteria grow only in inoculated chambers; the rest remain sterile (Fig. 2*A*). Moreover, FC40 stabilizes pinning lines sufficiently so that grids can be shaken without altering footprints (Movie S2). While we generally use FC40, the method works equally well with silicone and hydrocarbon oils; glass surfaces can also be used, as can polystyrene coated with cell-friendly materials (Fig. 2 *B*–*D*).

Varying Initial Chamber Volume. The volume of liquid initially in a chamber can be controlled in various ways. In one, different amounts of media are added during the first step; however, the interface has curvature and, hence, the fluid does not have an equal height across the dish. Therefore, it is convenient to use the approach in Fig. 2*E*: Three 6-cm dishes are covered with thin films plus blue dye, FC40 is added, and four lines are drawn in each to create three large central chambers (with volumes of

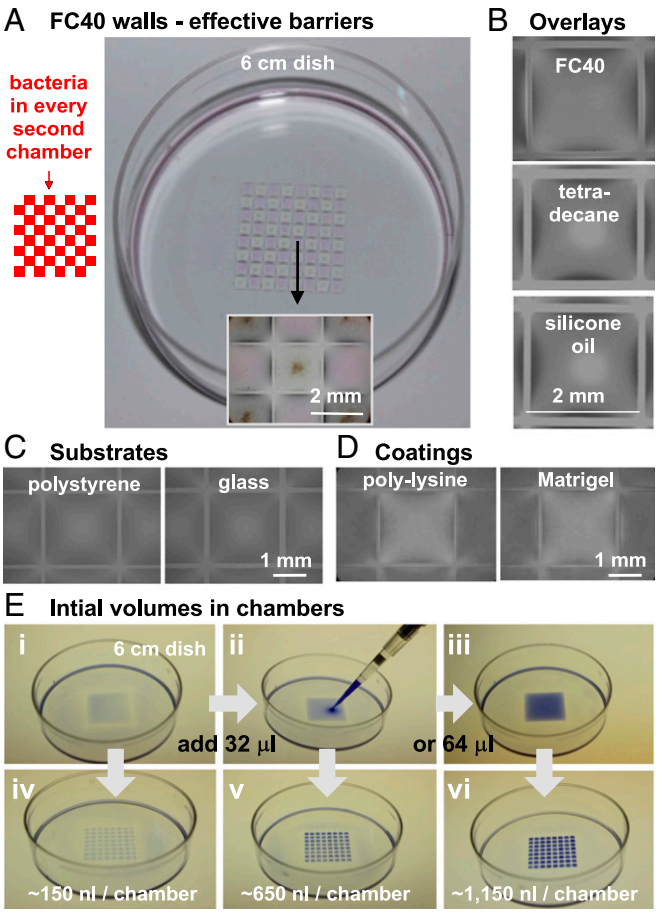

Fig. 2. Some different ways of making grids. (*A*) FC40 isolates chambers effectively. A 1.5 µL portion of medium ± *E. coli* was pipetted manually into every second chamber in an 8 × 8 grid (pattern shown in cartoon), with 2 × 2 mm chambers. After incubation (24 h; 37 °C), a phase-contrast image was collected. Bacteria grew only in inoculated drops (seen as aggregates in chambers containing exhausted, slightly yellow media), and the rest remained sterile (slightly-pink chambers). (*Inset*) Aggregates and granularity indicate presence of bacteria. (*B–D*) Various overlays and substrates yield stable pinning lines. Films of media on polystyrene (uncoated except in *D*) or on glass (*C*) were overlaid with 2 mL of FC40 (or other oils in *B*), grids were created, and phase-contrast images were collected. (*E*) Preparing grids with different starting volumes (2.25 × 2.25 mm chambers). (*i–iii*) Three dishes were covered with medium plus blue dye, FC40 was added, four 20-mm lines were drawn to create one central square in each dish (volume ~ 10 µL), and 0, 32, or 64 µL was pipetted into squares. (*iv–vi*) Subdivision yields grids.

~10 µL) to which more media plus dye are added (i.e., 0, 32, or 64 µL); lastly, the now-different volumes are split into three grids. Each of the 64 chambers in the three dishes ends up with ~150, ~650, or ~1,150 nL.

Essentially, all grids illustrated here are made by passing the stylus down the centerline of a large square or rectangle to divide them symmetrically into two; next, repeated symmetrical divisions (*SI Appendix*, Fig. S2 *A*, *i*) yield chambers with equal footprints and volumes. This is demonstrated using fluorescein instead of blue dye: chambers in a grid end up with similar fluorescence intensities, so volumes (chambers in *SI Appendix*, Fig. S2 *A*, *ii*) have a volume of 850 nL ± 4% (SD) (see *SI Appendix*, Fig. S2 for additional results, the calibration method, and reproducibility in a repeat experiment). However, if the stylus passes asymmetrically through a chamber offset from the centerline, the resulting sub-chambers can end up with very different volumes (in *SI Appendix*, Fig. S2*B*, they have 100 to 1,000 nL in an 8 × 8 grid).

Adding and Removing Liquids. Liquids can be delivered to conventional wells and to our chambers in the same way: by immersing a pipet tip into a recipient well/chamber (Fig. 1 *D*, *ii*). However, when repeating this process with the same pipet, liquids can be carried over from one well/chamber to the next, so pipets are usually washed or replaced between deliveries. Therefore, we investigated methods not requiring washing or replacement. In our printer, the pipet is a stainless steel tube mounted next to the stylus on a three-axis traverse. In one method, the pipet tip was positioned in the FC40 above a recipient chamber, and liquid was ejected into it through a transient "liquid bridge" (Fig. 3*A*). Because the pump driving ejection starts and stops and the tip moves down, up, and across, we call this "discontinuous" delivery. This method has been used to deliver one liquid to many chambers without carryover (20). Fig. 3*B* and Movie S3 illustrate a liquid bridge without detectable upward transfer of red dye from recipient chamber to delivering pipet that could cause carryover. We

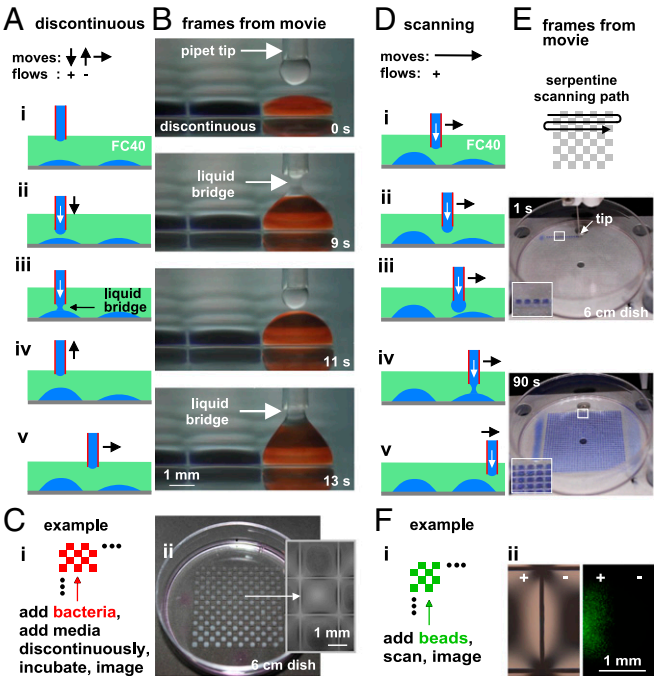

Fig. 3. Adding liquids discontinuously and continuously. (*A*) Discontinuous. (*i–iii*) The pipet is lowered (black arrow), and the pump ejects liquid (white arrow) that eventually merges with the chamber. (*iv, v*) After stopping the pump, the pipet is raised and moves to the next chamber. (*B*) Frames from Movie S3 illustrating that no red dye moved up through a liquid bridge to the pipet. Note that contact angles at the centers of chamber edges are ~90°. (*C*) Lack of carryover of bacteria during discontinuous delivery (2 × 2 mm chamber, ~150 nL). (*i*) A 300-nL portion of LB with or without ~20,000 *E. coli* was added manually to every second chamber, and then 500 nL of LB was added to all chambers by discontinuous delivery. (*ii*) After 3 d at 20 °C, imaging shows that bacteria (white) grew only in inoculated chambers. (*D*) Continuous (scanning). (*i–iii*) The pipet maintains a constant height (450 µm) above the substrate as it traverses (black arrow), continuously ejecting liquid (white arrow). (*iv*) Liquid is delivered to the chamber. (*v*) Continuing traverse breaks the liquid bridge (maximum final chamber height 380 µm). (*E*) Frames from Movie S4. The tip scans (15 mm/s) along a serpentine path, delivering ~70 nL of medium plus blue dye to each chamber. *Insets* show 4× magnifications. (*F*) No carryover of fluorescent beads between chambers during scanning (16 × 16 grid, 2 × 2 mm chambers, ~150 nL). (*i*) A 300-nL aliquot of medium with (+) or without (–) 9,000 fluorescent beads (1-µm diameter) was added manually to every second chamber in the grid. A total of 500 nL of medium was added by scanning to each chamber. (*ii*) Phase-contrast (*Left*) and fluorescent (*Right*) images showing that no beads were carried over between chambers.

demonstrated lack of carryover in another way. Bacteria were inoculated into every second chamber in a grid, and medium was delivered discontinuously into all chambers using the same tip (Fig. 3 *C*, *i*); on incubation, bacteria grew only in inoculated chambers while the others remained sterile (Fig. 3 *C*, *ii*). This confirms that bacteria are not carried over when medium is delivered, and that FC40 provides a sterile barrier between chambers.

With grids, there are no solid walls, and so no need to raise or lower the pipet as it traverses or to start and stop a pump. Consequently, one liquid can be delivered to many chambers by a pipet as it moves at constant speed and height, ejecting liquid continuously (Fig. 3*D*). Such "scanning" can deliver ~70 nL to each of 1,024 chambers in 90 s (Fig. 3*E* and Movie S4). The variation in delivery to a 16 × 16 grid (measured as in *SI Appendix*, Fig. S2) was 27 nL; it was 10 nL to a 32 × 32 grid (*SI Appendix*, *Materials and Methods*). Such delivery occurs without detectable carryover, exemplified by failure to transfer fluorescent beads between chambers (Fig. 3*F*). This illustrates another advantage of fluid walls: one liquid can be delivered through one tip speedily to many chambers without carryover because FC40 always remains in contact with the tip.

Our chambers have square footprints, and contact angles vary around the footprint (*SI Appendix*, Fig. S3). Therefore, we estimate maximum volumes that can be added to chambers based on scaling relative to a sessile circular drop with θ_A of 70° and θ_R of 3° (values for media without serum) and diameter equal to chamber width. Thus, a 1-mm square chamber in Fig. 1*B* is limited to minimum and maximum volumes of 4 and 120 nL, respectively (*SI Appendix*, Table S1 gives working volumes for chambers with different footprints; all are conservative estimates, as adding serum to medium increases θ_A).

Biocompatibility—Cells and Organisms. Grids are made using bioinert components: tissue-culture media and polystyrene dishes used by biologists, plus FC40. To confirm biocompatibility, a grid was prepared, NM18 cells (a line of mouse mammary tumor cells) were plated by scanning, and the dish was placed in a conventional CO_2 incubator (O_2 and CO_2 exchange freely through FC40); cells grew normally (Fig. 4*A*), as have all cells tested to date. Manipulations used in conventional tissue culture are easily adapted to grids, including feeding, trypsinization, replating (Fig. 4 *A* and *B*), and cloning (see *Example of a Complex Cell-Based Workflow—Genome Editing*). Cells can be grown on polystyrene or glass, and on polystyrene dishes coated with polylysine, Matrigel, collagen, fibronectin, and laminin (Fig. 2*D* and *SI Appendix*, Fig. S4 *A* and *B*). Cells can be adherent or nonadherent (*SI Appendix*, Fig. S4 *B* and *C*). They can also be cryopreserved in grids (Fig. 4*C*), as in conventional microfluidic devices (21, 22); this shows that these pinning lines are stable, which is remarkable, given the complex effects occurring when oil–water emulsions are frozen and thawed (23–25). Thus far, fluid walls have been made before adding cells; however, they can also be built around preplated cells (Fig. 4*D*). Consequently, fluid walls can be built around cells of particular interest already growing in a dish, so those with a characteristic morphology or expressing a particular fluorescent marker can be isolated. Note that here, the microfluidic pattern was modified during use, which is impossible with most microfluidic chips. Note also that FC40 provides an additional line of defense against contamination, as it is impermeable to bacteria (Fig. 3*C*). These experiments show that the standard procedures required for mammalian cell culture can be carried out in grids using submicroliter volumes.

We next demonstrate that whole organisms develop normally. *Caenorhabditis elegans* is a roundworm ~1 mm long that swims by undulatory locomotion; dorsal and ventral muscles contract alternately to generate waves along the worm's axis (26). Worms have been studied in conventional microfluidic devices (27) and droplet-based systems (28). We wished to see whether pinning

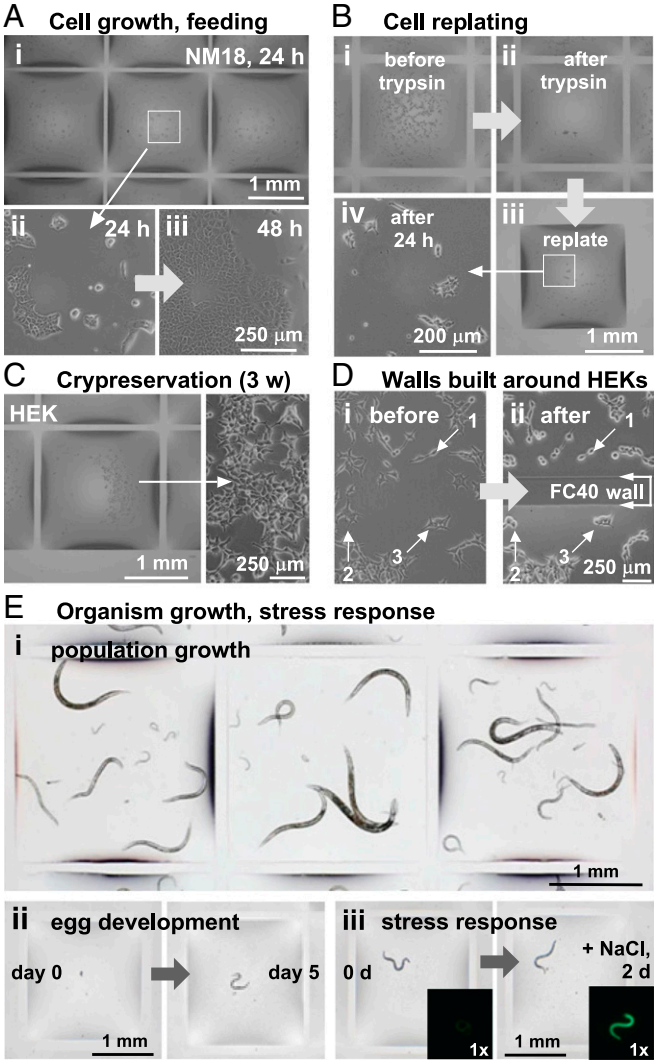

Fig. 4. Biocompatibility (2 × 2 mm chambers, initial volume 150 nL). (*A*) Growth and feeding. (*i*) A total of 250 NM18 cells in 800 nL were added to chambers by scanning, grown (24 h), fed (800 nL removed and 800 nL fresh medium added), and imaged. (*ii*) High-power view of selected region. (Magnification: 20× objective.) (*iii*) Cells were regrown (24 h) and reimaged, revealing that the cells grow normally. (*B*) Trypsinization and replating. (*i*) A total of 500 HEK cells in 500 nL are plated by scanning, grown (24 h), and imaged. (*ii*) After trypsinization, 1 μL is retrieved, and the chamber is reimaged; most cells have been removed. (*iii*) Retrieved cells were deposited in a new chamber, and this chamber was imaged. (*iv*) After growth (24 h), imaging confirmed successful cell transfer. (*C*) Cryopreservation. HEK cells are cryopreserved in grids for 3 wk at −80 °C, thawed, and regrown (24 h). Pinning lines and cells survive freezing and thawing. (*D*) Creating fluid walls around growing cells. (*i*) HEK cells (2×10^6) are plated, grown (24 h), and imaged. (*ii*) A grid was prepared around these adherent cells, and the same region of the dish was reimaged. A fluid wall divides the field; cells 1, 2, and 3 remain in their original positions as others in the path of the stylus are moved. (*E*) *C. elegans* develops and responds to osmotic stress normally. (*i*) Frame from Movie S5 illustrating worms living in a grid. (*ii*) Single eggs in 500 nL of S medium were deposited manually in chambers and fed daily; after 5 d, the resulting adult was imaged. (*iii*) Individual trauma-sensitive worms (strain CB7317) in 500 nL of S medium were deposited manually in chambers, and 500 nL of medium plus bacteria with or without 600 mM NaCl was added; after 2 d, worms were imaged. This strain expresses GFP in response to osmotic stress, and worms exposed to 300 mM NaCl fluoresce green. (*Insets*) Fluorescence images.

lines are strong enough to withstand swimming forces: they are (Fig. 4 *E*, *i* and Movie S5). After pipetting individual eggs manually into chambers, followed by food (i.e., bacteria), eggs

developed normally into adults (Fig. 4 *E*, *ii*). Worms also responded as expected to stress. Individuals of a strain (29) that expresses the green fluorescent protein (GFP) in response to trauma were grown with or without 300 mM NaCl; osmotic stress induced GFP expression (Fig. 4 *E*, *iii*). These experiments confirm biocompatibility, plus the strength and excellent optical properties of fluid walls.

Reconfiguring Fluid Walls—Antibody Labeling. We next show that fluid walls can be removed and rebuilt in the same place (Fig. 5 *A*, *i*). After plating in grids, NM18 cells were fixed, and the dish was removed from the printer, emptied of FC40, and washed with PBS; this destroys wall integrity, although some FC40 can remain pinned along initial footprints. After mounting the dish back on the printer, fluid walls were rebuilt in their original positions, although they can be built in different places if required.

Because breaking/making fluid walls is so easy, we incorporated it into an immunolabeling workflow. NM18 cells were induced by transforming growth factor β1 (TGF-β1) to reorganize their cytoskeleton and undergo the epithelial-to-mesenchymal transition (EMT; ref. 30). NM18 cells in some chambers were treated with TGF-β1 and fixed, and then the workflow involved cycles of destruction of fluid walls (when cells in all chambers are batch-washed, and, in one case, permeabilized) and wall rebuilding (so different reagents can be added to selected chambers; *SI Appendix*, Fig. S5). After finally remaking walls, cells were imaged. Cell morphology and fluorescence were as expected: TGF-β1 increased actin bundling (detected by phalloidin labeling) and vimentin expression (detected by immunolabeling)—two markers of the EMT (Fig. 5 *A*, *ii*). This confirms the self-healing properties of walls (they were pierced and resealed eight times) and demonstrates that immunolabeling can be performed in grids. This approach can be scaled to screen hundreds of antibodies with considerable cost savings while accelerating the workflow.

Pinning Lines Can Withstand Detergents—RT-PCR. A common cell-based workflow involves lysing cells with detergents, followed by RT-PCR to measure mRNA levels. We expected this would be impossible, as detergents reduce interfacial tension and destabilize pinning lines. However, it turns out that footprints in chambers made with medium plus serum are stable (Fig. 5 *B*, *i* and *ii*). We illustrate this using HEK cells that encode a GFP reporter gene controlled by a promoter switched on by tumor necrosis factor alpha (TNF-α): When exposed to the cytokine, cells fluoresced green (14) (Fig. 5 *B*, *iii*) and RT-PCR confirmed levels of GFP mRNA increase (Fig. 5*B*, legend). This shows that pinning lines can withstand destabilizing effects of detergents, presumably due to denaturation/cross-linking of serum components.

Example of a Complex Cell-Based Workflow—Genome Editing. We next performed a complex workflow: editing the *Casp6* gene using CRISPR-Cas9 (31, 32) (Fig. 6*A*). Here, NM18 cells growing in grids were transfected with an empty plasmid or with plasmid 880 or 881, which encodes Cas9 and a puromycin-resistance gene plus a guide RNA targeting a region of *Casp6*. After adding puromycin, cells were grown for 4 d; puromycin killed untransfected cells (which lack the resistance gene), whereas roughly half of the transfected ones remained alive (indicative of high transfection rates; *SI Appendix*, Fig. S6*B*). Cells were then transferred from chambers to conventional plates and expanded, and single cells were plated in new chambers. Some chambers received one cell (Fig. 6*B*), others received two, and some received none (based on the Poisson distribution). Many single cells grew into colonies (cloning efficiency 71%; Fig. 6*B* legend). The printer then picked clones and transfered them to microcentrifuge tubes. After expanding clones conventionally, followed by DNA amplification and sequencing, clones were found to have deletions at appropriate target sites (Fig. 6*C*); they also no longer expressed

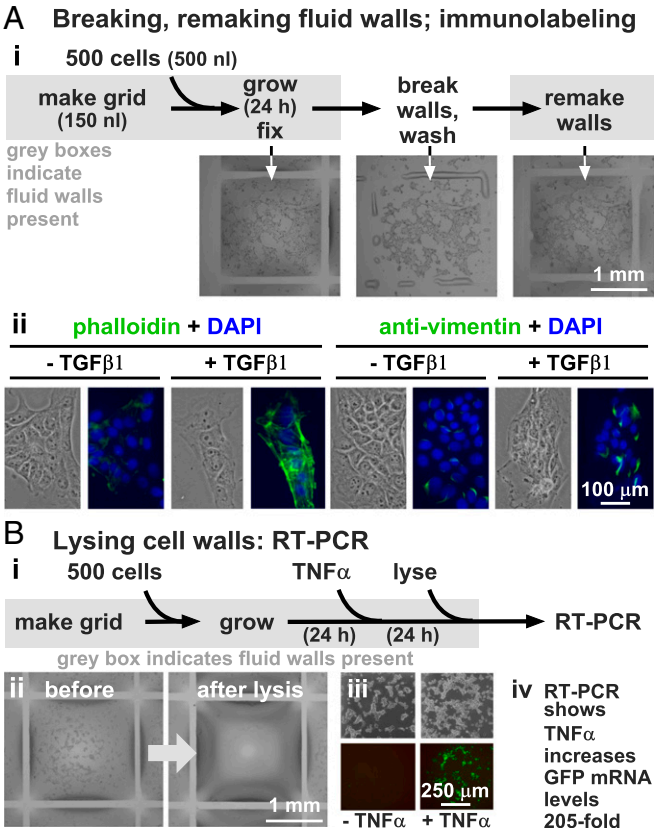

Fig. 5. Rebuilding fluid walls and destroying cell walls (2 × 2 mm chambers). The 6-cm dishes were mounted in positioning rings (tightly fitting circular sleeves enabling a dish plus ring to be removed from a printer and remounted so that walls can be rebuilt in the same place). (*A*) Breaking and remaking fluid walls during immunolabeling. (*i*) NM18 cells were plated by scanning, grown, and fixed; fluid walls were broken, all cells batch permeabilized with Triton X-100, and walls remade. Fluid walls survive fixation but are destroyed by emptying the dish of FC40 and washing with PBS (some FC40 remains pinned to the dish). After returning the dish to the printer and overlaying FC40, fluid walls are rebuilt. (*ii*) Cells respond to TGF-β1 as expected. The workflow involves cycles of making and destroying fluid walls (*SI Appendix*, Fig. S5); when walls are present, individual chambers are treated differently, and when walls are absent, all cells in all of the different parts of the dish are treated similarly. Cells were seeded by scanning in chambers, grown with (+) or without (–) TGF-β1, and then fixed. Next, walls were destroyed, fixative was washed away, cells were permeabilized, walls were rebuilt, phalloidin or anti-vimentin (both conjugated with Alexa 488) was added to selected chambers, walls were destroyed, cells were washed, walls were rebuilt, DAPI was added, walls were destroyed, cells were washed, walls were rebuilt, and phase and fluorescent images were collected. TGF-β1 induces actin bundling and increases vimentin expression (detected by phalloidin labeling and immunolabeling, respectively). (*B*) Lysing cells and RT-PCR. (*i*) HEK-293 reporter cells were plated by scanning in chambers and then grown (24 h), medium with (+) or without (–) TNF-α (10 ng/mL) was added, cells were regrown (24 h) to allow the cytokine to induce GFP expression before washing and lysis, and lysates were transferred from chambers to microcentrifuge tubes for assessment of levels of GFP mRNA by RT-PCR. (*ii*) Pinning lines survive lysis. (*iii*) Phase-contrast (*Top*) and fluorescence images (*Bottom*) show TNF-α induces GFP expression. RT-PCR also showed that TNF-α increases GFP mRNA levels 205-fold (lower and upper bounds: 174- and 241-fold), normalized relative to the control (lower and upper bounds: 0.63- and 1.6-fold; $n = 4$).

Casp6 protein (*SI Appendix*, Fig. S6*C*). Here, walls were pierced 16 times, and pinning lines survived treatment with transfection reagent. Significantly, fluid walls provide excellent optical clarity; there are no solid walls to obscure the view (in contrast to cloning in conventional flat microplates, where cells often sit

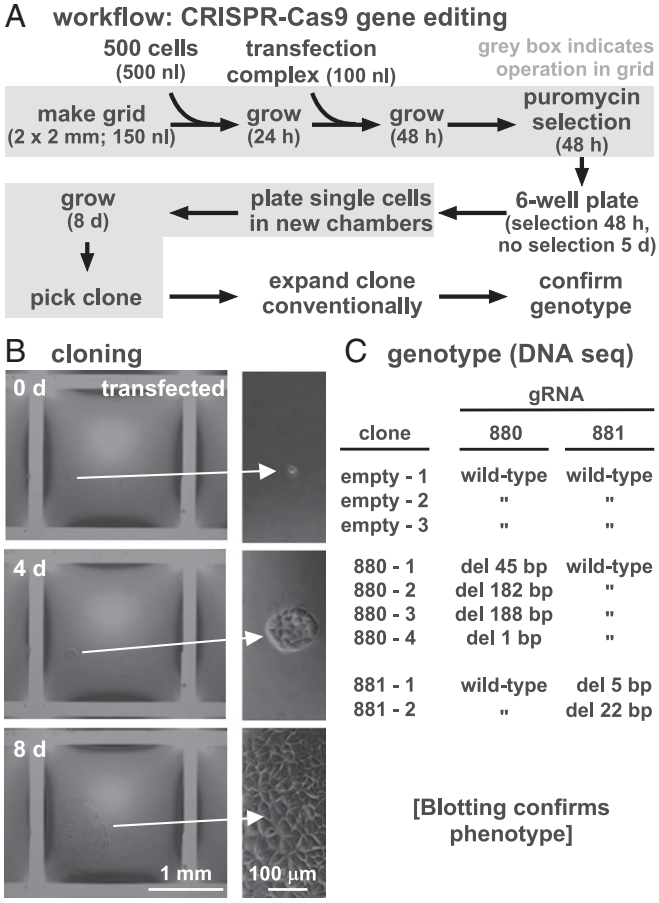

Fig. 6. A complex workflow: deriving a NM18 cell clone with a mutated *Casp6* gene using CRISPR-Cas9. (*A*) Workflow. Cells were transfected with empty vector (encoding Cas9 plus puromycin resistance) or with plasmid 880 or 881, which additionally encode a guide RNA (gRNA) targeting different parts of *Casp6*. (*B*) Cloning. After transfection, puromycin selection (*SI Appendix*, Fig. S6), and expanding the cells conventionally, the printer delivered ∼0.2 cells (by scanning) to each chamber; images show the single cell divides over 8 d. Initially, 42 of 256 chambers (40 expected from Poisson distribution) contained one cell; after 8 d, 30 had colonies (71% cloning efficiency). (*C*) Genotyping. After picking colonies (as in Fig. 4*B*), the printer delivered the cells to a microcentrifuge tube. Cells were then expanded conventionally, DNA was purified, the *Casp6* region was amplified by PCR and cloned in bacteria, and genotypes were determined by sequencing. Clones derived from transfections with plasmids 880 and 881 have deletions (del) in expected regions, unlike those receiving empty vector. Immunoblotting confirmed the phenotype (*SI Appendix*, Fig. S6).

against surrounding walls and "edge effects" prevent them from being seen clearly). Moreover, when cells are seeded centrally in grids, fluid dynamics and chamber geometry ensure that few end up near pinning lines; preexisting (cell-free) medium is forced by incoming cell-containing medium toward edges (*SI Appendix*, Fig. S7). Consequently, users can have confidence in monoclonality. Since growing clones can be identified earlier, they can be picked sooner (in Fig. 6*C*, after 8 d, which contrasts with >14 d in conventional plates).

Discussion

We describe a microfluidic platform for miniaturizing workflows in cell biology. Grids are made by covering the surface of a Petri dish with a thin layer of medium, overlaying FC40, and using a Teflon stylus to reshape the aqueous phase into an array of individual chambers; each chamber is isolated from neighbors by liquid walls of FC40 (Fig. 1 *A*–*C*). At the microscale, effects due to gravity and buoyancy are negligible, and the aqueous phase remains pinned to the plastic; consequently, such grids can be used much like conventional microplates—liquids are simply pipetted through FC40 instead of air (Fig. 1*D*).

During fabrication, this platform has many advantages compared with other methods. It does not require a dedicated facility or specialized equipment beyond a syringe pump and an automated positioning system to drive the stylus; thus, fluid walls/ceilings are built accurately, reproducibly, and immediately by interfacial forces (e.g., our stylus generally traverses at 25 mm/s and builds 256 and 1,024 chambers in a 6-cm dish in ∼2 and ∼4 min, respectively; Movie S1). Building is scalable; for example, the array in Fig. 1*C* has a chamber density equivalent to a microplate with 393,216 wells. High-density grids are created efficiently (drawing twofold more lines yields fourfold more chambers), and ∼90% of the surface area is available for cell culture in contrast to ∼40% in a conventional 1,536-well plate (*SI Appendix*, Fig. S1*B*, calculated assuming fluid walls are 100 µm wide).

During use, there are additional advantages. First, pinning lines are stable, and fluid walls pliant and resilient. They withstand agitation (Movie S2), they morph above unchanging footprints when liquids are added/removed (Fig. 1 *D*, *v*), and self-heal when pipets are inserted through them (in Fig. 6, walls were pierced 16 times). Second, uniform volumes can be added to many chambers quickly and easily; because there are no solid walls, there is no need to raise/lower and/or wash the delivering pipet or to start/stop the pump. Instead, one pipet can scan through FC40 at constant speed and height, ejecting liquid continuously to feed chambers through transient liquid bridges. Such scanning can deliver 70 nL to each of 1,024 chambers in 90 s without detectable carryover (Fig. 3*E* and Movie S4). Third, all points in the aqueous phase are accessible. Fourth, walls confining the aqueous phase can be reconfigured during use; for example, new walls can be added (Fig. 4*D*) and existing ones destroyed and then rebuilt in the same place (Fig. 5*A*).

The platform has another significant advantage: It is biocompatible if used with the culture media and dishes (including coated ones; *SI Appendix*, Fig. S4 *A* and *B*) familiar to biologists, along with what is arguably the most bio-inert immiscible liquid available—FC40 (17–19). Cells (from bacteria to humans) grow normally in grids (Figs. 2*A*, 3*C*, and 4 *A* and *B*), worm eggs develop into adults (Fig. 4 *E*, *ii*), and cells/organisms respond as expected to stimuli (stress, puromycin, TGF-β, and TNF-α; Figs. 4 *E*, *iii* and 5). We also miniaturize the basic manipulations involved in mammalian cell culture (e.g., feeding, replating, cryopreservation, cloning; Figs. 4 *A*–*C* and 6*B*) and some widely used downstream workflows (fixation and immunolabeling; cell lysis and RT-PCR; and transfection and genome editing; Figs. 5 and 6). Because walls can be built around living cells of interest (Fig. 4*D*)—perhaps ones with characteristic morphologies or expressing particular fluorescent markers—selected cells can easily be isolated from others (for subsequent growth or analyses) without touching them. We also anticipate that grids will prove especially useful for cloning. With conventional microplates, single cells often sit against surrounding walls and cannot be imaged clearly because of edge effects. In contrast, fluid walls lack obscuring walls and thus yield excellent optical clarity. In addition, because cells are deposited centrally in chambers, and fluid dynamics and geometry ensure that few end up at the edges of footprints (*SI Appendix*, Fig. S7), users can be confident about which chambers contain only one cell. Moreover, clones can be picked sooner (e.g., after 8 d in Fig. 6*B*). Additionally, FC40 provides an extra barrier to contamination, isolating each chamber from others in one dish and from the external world (Fig. 2*A*).

As with any platform, ours has limitations. First, an immiscible liquid is required to limit evaporation (as is generally the case wherever submicroliter volumes are handled). Second, liquids and surfaces must be matched to ensure that pinning lines are stable. We use the following approach to test new combinations

rapidly: A drop of aqueous liquid is placed on the substrate and overlaid with FC40, and most of the aqueous phase is removed. If pinning lines do not retract, then the combination can probably be used. Third, there are limits to upper and lower volumes that chambers can accommodate without change in footprint. These limits depend on advancing and receding contact angles; for example, with the angles of 70° and 3°, respectively, a 2 × 2 mm chamber has working volumes of 35 to 1,100 nL, and a 140 × 140 μm chamber has working volumes of 9 to 270 pL (*SI Appendix*, Table S1).

In summary, we have developed a versatile platform for fabricating microfluidic patterns, exemplified by making arrays of square chambers with nanoliter volumes. These grids are used like conventional microplates, except that liquids are pipetted through FC40 instead of air. We anticipate that they will prove especially useful in cell biology, as they are made with materials familiar to users, can be incorporated into common workflows, and provide considerable savings in consumables.

Materials and Methods

General Reagents and Equipment. FC40 was purchased from Acota. It is bioinert, not found in regulatory lists of dangerous organic chemicals (33), and it should not be confused with the volatile chlorofluorocarbons that release the chlorine radicals destroying the ozone layer. If grids are to be kept for days, extra FC40 should be added when needed (14). Evaporated FC40 has had no untoward effects on any of many different cell types grown conventionally in the same incubator at the same time over 3 y. All other fluids and materials were from Sigma-Aldrich unless otherwise stated. Where indicated, aqueous drops contain water-soluble dyes (e.g., Allura Red, toluidine blue, resazurin).

Most grids were fabricated, and small volumes delivered to them, using an isoCell (Iota Sciences Ltd). This is essentially a tool-head driven by a three-axis traverse and appropriate software; the tool-head holds a stylus—a Teflon rod (3.8-mm diameter) with a conical tip (angle at tip ∼50°)—and a stainless steel dispensing needle (width 0.5-mm o.d.) connected to a syringe pump. This Teflon stylus was used to make all grids, except for ones shown in Fig. 1 *C* and *D*, *v*, Fig. 3, and *SI Appendix*, Fig. S1 *B* and *C*, where the rod was replaced by a Teflon tube (o.d. ∼750 μm; Cole Parmer). As the dispensing needle is hydrophilic, liquid can run up the outside instead of into a chamber as wanted, and this both makes accurate delivery of small volumes unreliable (34) and increases carryover contamination when delivering one liquid to many chambers in a grid from one dispensing tube. Therefore, a hydrophobic sleeve (a piece of Teflon tubing) is included around the tip of the dispensing tube to prevent runback (Movie S4). The central workplace holds a 6-cm dish, plus microcentrifuge tubes containing reagents (often tissue-culture media, 70% ethanol for sterilization; Movie S4). The 6-cm dish is placed in a positioning ring—a tightly fitting circular sleeve bearing a protrusion that ensures the dish plus ring can be mounted, removed, and remounted in the isoCell workplace in the same orientation. Where sterility is required, the printer is placed in a bio-safety cabinet, and sterile procedures used throughout (e.g., the stylus tip is sterilized with 70% ethanol, and the software includes cycles for aspirating 70% ethanol into the tube connected to the dispensing needle and ejecting the ethanol into a waste tube). When printing grids on rectangular flat (one-well) polystyrene microtiter plates (127.7 × 85.5 mm; Nunclon; Thermo Fisher Scientific), the 3D-traverse system described by Walsh et al. (14) fitted with a stylus (a Teflon tube) was used.

Printing and Operation of Grids. Grids were generally fabricated using the isoCell and 6-cm polystyrene tissue culture dishes [60-mm Falcon TC-treated cell culture dish (product #353002) and 60-mm Corning TC-Treated Culture Dish (product #430166)]; these dishes have internal diameters of ∼5 cm. The 6-cm dishes were coated, where stated, with polylysine, Matrigel (Corning), fibronectin, laminin, or collagen (Cell Applications Inc.) by covering the bottom of the dish with the liquid coating using the concentrations, times, and temperatures suggested by the manufacturer (except for collagen, see below); removing most of the liquid coating to leave a thin film on the surface; and (without allowing the coating to dry) immediately adding DMEM plus 10% FBS and creating grids. For collagen, a 0.5× dilution (2.5 $\mu g/cm^2$) was used, as the thicker coating prevented FC40 from wetting the surface. Glass substrates were either glass microscope slides/coverslips in 6-cm dishes, or 35-mm glass bottom dishes (No. 0; MatTek). DMEM plus 10% FBS was used to make all grids described, except those for use with worms; when the term "medium" is used in the context of mammalian cell culture, it should be assumed that serum is present unless stated otherwise. Typically, 1 mL DMEM plus 10% FBS is pipetted manually into a 6-cm dish, medium swirled around so the bottom is covered completely when the dish is horizontal, the dish tilted, and 0.9 mL medium removed and discarded. The bottom is now completely covered by a thin film of medium. A 3-mL aliquot of FC40 is manually pipetted into the dish so that a layer of FC40 covers the medium. Steps before overlaying FC40 are carried out quickly if the grid is to be used with cells so that the pH of the medium remains unchanged. After placing the dish in the work area on the printer, the system uses in-built software to "home" the tool head, select the stylus, "draw" lines to create the grid (stylus speed typically 25 mm/s), deselect the stylus, and go "home". Additionally, the software can select a pipet (the "pen"), deliver nanoliter volumes to selected chambers (by switching on and off an in-built syringe pump), deselect the stylus, and go "home".

Detailed methods for individual figures are described in *SI Appendix, Materials and Methods*.

ACKNOWLEDGMENTS. We thank Jonathan Hodgkin, Hayley Lees, Alison Woollard, and Joey Riepsaame for help. This work was supported by Iota Sciences Ltd. (C.S., A.F., A.N.T., and H.W.), a Royal Society University Research Fellowship (to A.A.C.-P.), the Impact Acceleration Account of the Biotechnology and Biological Sciences Research Council (P.R.C. and E.J.W.), awards from the Medical Research Council under the Confidence in Concept scheme (MC_PC_15029 to P.R.C. and E.J.W. and MR/K010867/1 to P.R.C.), and a European Commission for a 7th Framework Marie Curie Career Integration Grant (Contract 333848 to E.J.W.).

1. Ng K, et al. (2017) Paper-based cell culture platform and its emerging biomedical applications. *Mater Today* 20:32–44.
2. Marcy Y, et al. (2007) Nanoliter reactors improve multiple displacement amplification of genomes from single cells. *PLoS Genet* 3:1702–1708.
3. Kim S-H, Lee GH, Park JW (2013) Microwell fabrication methods and applications for cellular studies. *Biomed Eng Lett* 3:131–137.
4. Liberski AR, Delaney JT, Jr, Schubert US (2011) "One cell-one well": A new approach to inkjet printing single cell microarrays. *ACS Comb Sci* 13:190–195.
5. Hoffmann J, Trotter M, von Stetten F, Zengerle R, Roth G (2012) Solid-phase PCR in a picowell array for immobilizing and arraying 100,000 PCR products to a microscope slide. *Lab Chip* 12:3049–3054.
6. Du G-S, et al. (2013) Cell-based drug combination screening with a microfluidic droplet array system. *Anal Chem* 85:6740–6747.
7. Shemesh J, et al. (2014) Stationary nanoliter droplet array with a substrate of choice for single adherent/nonadherent cell incubation and analysis. *Proc Natl Acad Sci USA* 111:11293–11298.
8. Berthuy OI, et al. (2016) Multiplex cell microarrays for high-throughput screening. *Lab Chip* 16:4248–4262.
9. Cole RH, et al. (2017) Printed droplet microfluidics for on demand dispensing of picoliter droplets and cells. *Proc Natl Acad Sci USA* 114:8728–8733.
10. Schmitz CH, Rowat AC, Köster S, Weitz DA (2009) Dropspots: A picoliter array in a microfluidic device. *Lab Chip* 9:44–49.
11. Shembekar N, Chaipan C, Utharala R, Merten CA (2016) Droplet-based microfluidics in drug discovery, transcriptomics and high-throughput molecular genetics. *Lab Chip* 16:1314–1331.
12. Prakadan SM, Shalek AK, Weitz DA (2017) Scaling by shrinking: Empowering single-cell 'omics' with microfluidic devices. *Nat Rev Genet* 18:345–361.
13. Sackmann EK, Fulton AL, Beebe DJ (2014) The present and future role of microfluidics in biomedical research. *Nature* 507:181–189.
14. Walsh EJ, et al. (2017) Microfluidics with fluid walls. *Nat Commun* 8:816.
15. Berthier E, Beebe DJ (2007) Flow rate analysis of a surface tension driven passive micropump. *Lab Chip* 7:1475–1478.
16. Berthier J, Brakke K (2012) *Physics of Microdroplets* (J Wiley and Sons, Hoboken, NJ).
17. Riess JG, Krafft MP (1998) Fluorinated materials for in vivo oxygen transport (blood substitutes), diagnosis and drug delivery. *Biomaterials* 19:1529–1539.
18. Greenspan JS, Wolfson MR, Rubenstein SD, Shaffer TH (1990) Liquid ventilation of human preterm neonates. *J Pediatr* 117:106–111.
19. Sarkar S, Paswan A, Prakas S (2014) Liquid ventilation. *Anesth Essays Res* 8:277–282.
20. Zhu Y, et al. (2014) Nanoliter-scale protein crystallization and screening with a microfluidic droplet robot. *Sci Rep* 4:5046.
21. Li L, Lv X, Guo H, Shi X, Liu J (2014) On-chip direct freezing and thawing of mammalian cells. *RSC Adv* 4:34443–34447.
22. Kondo E, Wada K, Hosokawa K, Maeda M (2016) Cryopreservation of adhered mammalian cells on a microfluidic device: Toward ready-to-use cell-based experimental platforms. *Biotechnol Bioeng* 113:237–240.
23. Kabalnow AS, Shchukin ED (1992) Ostwald ripening theory: Applications to fluorocarbon emulsion stability. *Adv Colloid Interface Sci* 38:69–97.
24. Sgro AE, Chiu DT (2010) Droplet freezing, docking, and the exchange of immiscible phase and surfactant around frozen droplets. *Lab Chip* 10:1873–1877.
25. Hauptmann A, Handle KF, Baloh P, Grothe H, Loerting T (2016) Does the emulsification procedure influence freezing and thawing of aqueous droplets? *J Chem Phys* 145:211923.
26. Gray J, Lissmann HW (1964) The locomotion of nematodes. *J Exp Biol* 41:135–154.

27. Cornaglia M, Lehnert T, Gijs MAM (2017) Microfluidic systems for high-throughput and high-content screening using the nematode *Caenorhabditis elegans*. *Lab Chip* 17: 3736–3759.
28. Clausell-Tormos J, et al. (2008) Droplet-based microfluidic platforms for the encapsulation and screening of mammalian cells and multicellular organisms. *Chem Biol* 15:427–437.
29. Pujol N, et al. (2008) Anti-fungal innate immunity in *C. elegans* is enhanced by evolutionary diversification of antimicrobial peptides. *PLoS Pathog* 4:e1000105.
30. van Meeteren LA, ten Dijke P (2012) Regulation of endothelial cell plasticity by TGF-β. *Cell Tissue Res* 347:177–186.
31. Doudna JA, Charpentier E (2014) Genome editing. The new frontier of genome engineering with CRISPR-Cas9. *Science* 346:1258096.
32. Hsu PD, Lander ES, Zhang F (2014) Development and applications of CRISPR-Cas9 for genome engineering. *Cell* 157:1262–1278.
33. 3M Company (2017) 3M Fluorinert Electronic Liquid FC-40: Safety data sheet, version 12.01. Available at https://www.acota.co.uk/assets/downloads/data-centre/msds/3m/3M%20Fluorinert%20Electronic%20Liquid%20FC-40.pdf. Accessed May 6, 2018.
34. Dong Z, Ma J, Jiang L (2013) Manipulating and dispensing micro/nanoliter droplets by superhydrophobic needle nozzles. *ACS Nano* 7:10371–10379.